

GW electronic structure calculations of Co doped ZnO

Dennis Franke, Michael Lorke, and Thomas Frauenheim

Bremen Center for Computational Materials Science,

University of Bremen, Am Fallturm 1, 28359 Bremen, Germany

Andreia Luisa da Rosa

Bremen Center for Computational Materials Science,

University of Bremen, Am Fallturm 1, 28359 Bremen, Germany and

Federal University of Goiás, Institute of Physics,

Av. Esperança, Campus Samambaia, Goiânia, Brazil

(Dated: today)

Abstract

Recently the point defect responsible for the emission of cobalt in doped ZnO samples has been identified [1]. In this work we further extend our investigation to other point defects in Co-doped ZnO. We use density-functional theory and GW calculations to determine the orbital-resolved band structure of cobalt doped zinc oxide (ZnO). We show that mainly O-p and Co-d orbitals take part in the process and confirm that an oxygen interstitial nearby a cobalt atom is a likely defect to occur in ion beam Co-doped ZnO samples. We also rule out that other common point defects in ZnO can be responsible for the observed d-d transition. Finally, we suggest that defect complexes involving oxygen interstitials could be used to promote ferromagnetism in cobalt doped ZnO samples.

Impurities in semiconductors offer the possibility of manipulating their electronic, magnetic and optical properties. Cobalt doped ZnO has attracted great interest for applications in diluted magnetic semiconductors (DMS)[2–11] and consequently can provide a way to possibly use the electron spin for quantum information devices [12, 13]. Furthermore, doping of ZnO with transition metals and rare-earths were found to extend the emission range from the intrinsic band gap to the infrared spectrum. Consequently, Co atoms can be incorporated as optical centers into the ZnO matrix, allowing to tune its electronic and optical properties, making it interesting for optoelectronic devices, for example as single-photon emitters [14, 15]. Intrinsic defects, such as vacancies or interstitials, forming defect complexes with the substitutional impurity can change the ionization state and coordination number of cobalt, which strongly affect the luminescence properties[16, 17].

Recent experiments have shown that after Co implantation, luminescence signatures at 1.74–1.88 eV have been observed [1, 18, 19]. Co is found to be incorporated at a zinc site leading to a 2+ oxidation state. Luminescence spectra of ZnO nanowires ensembles with nominal Co concentrations ranging from 0.05 to 8.0 at% after annealing in air at temperatures of 500-900°C shows luminescence in the visible region assigned to cobalt incorporation. The mechanism underlying this process has been recently identified by some of us [1] in which a defect involving a cobalt atom substituting a zinc atom nearby with an oxygen interstitial atom. In this work by employing state-of-the-art first principles calculations, we further explore the mechanism for this luminescence and extend our investigation to other defects to show that other common point defects can be rule out in participating in the observed d-d transition.

We employ density-functional theory [20, 21] and many-body GW methods [22] as implemented in the Vienna ab initio simulation package (VASP) [23] to investigate the electronic structure of Co-doped ZnO in the presence of intrinsic defects. The supercell used in the calculations consisted of 72 atoms with a Co concentration of 2.7%. The projected augmented wave method (PAW) has been used [23, 24] to relax the structures with the Perdew-Burke-Ernzenhof (PBE) form for the exchange-correlation functional [25]. A plane wave basis set with an energy cutoff of $E_{\text{cut}} = 400\text{eV}$ and a $(3 \times 2 \times 2)$ Monkhorst-Pack \mathbf{k} -point sampling was employed to integrate the charge density. GW calculations have been performed to determine the electronic structure of the doped systems. This approach has been successfully used in our previous works[1, 15, 26, 27].

Since the preparation conditions can be varied by providing a O-rich or Zn-rich environment, this can lead to drastic changes in the electronic structure of pure ZnO [1, 14, 28, 29]. Conse-

quently, it is expected that intrinsic defects would also influence the electronic properties of doped samples. In Fig. 1 the relaxed geometries of (a) Co_{Zn} (Co substitutional at a zinc site) is shown. Incorporating cobalt into the ZnO matrix at a substitutional sites does not cause significant strain in the ZnO lattice. The cobalt distances to nearest neighbour oxygen atoms are 1.97 Å and 1.98 Å for in-plane and c -direction, respectively. The Co-Zn distances are 3.29 Å for atoms in the basal plane and 3.23 Å along the c -direction. Fig. 1 (b) shows the relaxed geometry of a Co substitutional at a zinc site plus an oxygen interstitial nearby $\text{Co}_{\text{Zn}} + \text{O}_{\text{int}}$. The Co-O distances to nearest neighbour oxygen atoms in the ZnO lattice are 1.92 Å along the c and 1.94 Å for the in-plane direction. The distance to the oxygen interstitial is 1.73 Å. Although the overall change in the structural properties of ZnO is not significant, the change in the electronic structure of both systems compared to bare ZnO is clearly visible, as we discuss below.

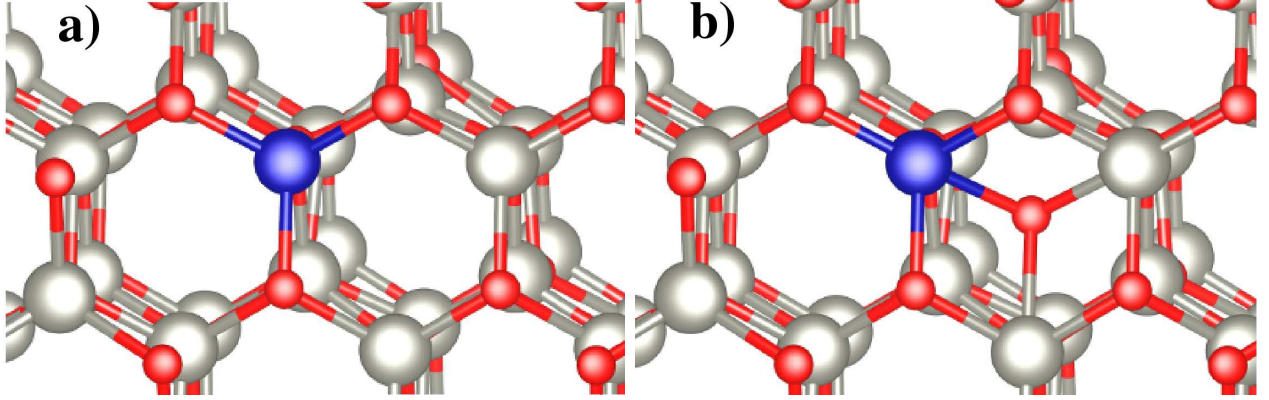


FIG. 1. Atomic structure around the a) Co_{Zn} and b) $\text{Co}_{\text{Zn}} + \text{O}_{\text{int}}$ defects calculated within the PBE functional. Grey, red and blue spheres represent Zn, O, and Co atoms, respectively.

The orbital decomposed electronic structure of Co_{Zn} and $\text{Co}_{\text{Zn}} + \text{O}_{\text{int}}$ defects is shown in Fig. 2. We first discuss the density-of-states of Co_{Zn} shown in Fig. 2(a). As Co ions occupy the Zn site in wurtzite ZnO, the ZnO octahedral crystal field splits the Co-3d states into lower e and higher t_2 levels. In the absence of other point defects, the majority-spin e and t_2 as well as the minority-spin e states are filled, while the minority spin down t_2 states are empty.

For Co_{Zn} shown in Fig. 2 (a) we can see that the Co- d states lie inside the band gap, around 2 eV above the VBM. In this configuration, Co has a formal charge of 2+. The d spin-up states are fully occupied, whereas the d spin-down orbitals are only partially occupied. The states labeled A close to the VBM (around -2 eV) are composed by O- p states and Co- d states, with larger contribution from Co- d_{z^2} states. The states B, close to Fermi level, are composed mostly by Co- $d_{x^2-y^2}$ and

Co- d_{xz} orbitals. The CBM (0.8-1 eV), as expected, is dominated by Zn-4s states eV. Further Co-t₂ states are seen inside the conduction band around 2-3 eV. States labeled C, are composed mostly by Co- $d_{x^2-y^2}$ and Zn-s orbitals. As a conclusion, there are no empty d-states inside the ZnO band gap or close to the CBM to promote the observed d-d transition. Therefore, we rule out that Co_{Zn} is responsible for the experimentally observed luminescence reported in Refs.[1, 18, 19].

Next we discuss the orbital projected density-of-states of Co_{Zn} + O_{int} shown in Fig. 2(b). States D, close to Fermi level, are composed mainly by Co- d_{yz} and O- p_z . The CBM located at E (region around 2 eV) shows mostly Co- d_{x^2} and O- p_x character. Higher states in the conduction band, between 3.2 and 3.8 eV, show overlap between Co- $d_{x^2-y^2}$ and O- p_z states. By comparing both Co_{Zn} and Co_{Zn} + O_{int}, it is clear that they possess very different electronic structures. The main contrast lies on the fact that the separation between the Co low-spin states e are very different. While for Co_{Zn} the splitting between e and t₂ states is 3.2 eV, for Co_{Zn} + O_{int} it is 2.4 eV. This means that the separation between these states is reduced in the presence of and oxygen interstitial and therefore the overlap between Co-d and Zn-4s states is enhanced. As reported previously, these results are in very good agreement with the experimentally observed luminescence signatures at 1.88 eV and 2.02 eV [1, 18, 19].

In order to have further insight on the localization of these states, the corresponding band projected charge densities calculated within the PBE+GW₀ approximation are shown for both Co_{Zn} (Figs.5(a)-(c)) and Co_{Zn}+O_{int} (Figs.3(d)-(e)). Fig.3(a) shows the states located at A, Fig.3(b) shows the states close to the Fermi level at B, and Fig.3(c) shows the states located at C. All states are very localized around the Co atom, with little or negligible overlap with the ZnO matrix. It is evident that the states are strongly localized on the cobalt atom with only minor contributions on the neighboring oxygen atom for the Co_{Zn} defect. In contrast, the inclusion of the interstitial oxygen nearby leads to a different situation, with a stronger hybridization with the ZnO lattice. For Co_{Zn} + O_{int} Fig.3(d) show the states close to the Fermi level, Fig.3(e) shows states located at E and Fig.3(f) shows higher states in the conduction band located at F. Hence in the band projected charge densities for Co_{Zn} + O_{int} shown in 3(e) one can clearly see that the interstitial oxygen promotes leads to additional electrons in the band gap, making the $d-d$ transition possible.

Additionally, we have extended our investigation to Co-complexes involving other common point defects in ZnO [30–33]. First we discuss the relaxed atomic structure of these complexed in ZnO. When a zinc vacancy is close to a cobalt interstitial atom, Co_{Zn} + V_{Zn}, shown in 4(a) the Co atom slightly shifts towards the vacancy, resulting in two different Co-Zn distances along

the c -direction, namely 3.21 Å and 3.29 Å as well in the basal plane, 3.27 Å and 3.30 Å. The Co-O bonds are 1.79 Å and 1.90 Å in the basal plane and 1.94 Å along the c -direction. The next investigated structure is an oxygen vacancy close to a cobalt interstitial atom, $\text{Co}_{\text{Zn}} + \text{V}_{\text{O}}$ shown in 4(b). The presence of the vacancy does not disturb the lattice strongly. The Co-O distances is 1.96 Å. Co-Zn distances are 3.27 Å along the basal plane and 3.29 Å along the c -direction. The optimized geometry for a complex involving a zinc interstitial and a cobalt substitutional atom complex $\text{Co}_{\text{Zn}} + \text{Zn}_{\text{int}}$ is presented in Fig. 4(c). The zinc interstitial atom disturbs the lattice and consequently the cobalt atom relaxes outwards. The distances between the Co interstitial and its nearest-neighbour oxygen atoms lie in the range 1.69-2.20 Å. This leads to Co-O distances of 2.00 Å in the basal plane and 2.06 Å along the c -direction. The Co-Zn_i distance is 2.21 Å and Co to second nearest neighbours is 3.25 Å.

In order to verify whether any of these defects can also give rise to luminescence in ZnO, we have calculated their corresponding total and Co-projected density of states as shown in Fig. 5. For $\text{Co}_{\text{Zn}} + \text{V}_{\text{Zn}}$, Fig. 5(a), there are no empty Co- d states inside the band gap and the formal charge of the Co atom is close to 3+. Occupied states are located at the VBM and 1 eV above it. Therefore we conclude that this defect complex cannot be responsible for the experimentally observed red emission. The electronic structure for the $\text{Co}_{\text{Zn}} + \text{V}_{\text{O}}$ structure is displayed in Fig. 5(b). Since there are no intra-gap states stemming from the Co atom this defect cannot be responsible for any luminescence observed in the experiment. Finally, the density of states for $\text{Co}_{\text{Zn}} + \text{Zn}_{\text{int}}$ is shown in Fig. 5(c). Intra-gap states are now present, with empty states located at -2.5 and -0.3 eV and occupied states are located at 0.4 and 1.2 eV. The Co formal charge is close to 2+. However, no clear optical transition is seen.

In order to assess the thermodynamic stability of defect complexes, we have calculated their formation energies. Following the approach described in Ref. [34], the formation energy E_{f} of a neutral defect in ZnO is defined as

$$E_{\text{f}} = E_{\text{defect}}^{\text{tot}} - E_{\text{bulk}}^{\text{tot}} - \sum_i n_i \mu_i, \quad (1)$$

where $E_{\text{defect}}^{\text{tot}}$ is the total energy of the respective defect complex and $E_{\text{bulk}}^{\text{tot}}$ is the total energy of a bulk ZnO supercell. n_i describes the number of atoms of type i that have been added or removed from the complex with μ_i as the corresponding chemical potential. Since the conditions can assume any value between Zn-rich or O-rich conditions in a synthetization process, limits

should be introduced to the chemical potential μ . In the lower limit, the material is free of defects, whereas the upper limit corresponds to the formation of elemental bulk/precipitation phases. This can be avoided by employing the following condition for Co metal $\mu_{\text{Co}} \leq \mu_{\text{Co-bulk}}$. A similar condition can be imposed for cobalt oxide in order to avoid the formation of such crystal phases $\mu_{\text{Co}} \leq \mu_{\text{CoO}}$, where CoO was chosen as the upper limit. With μ_{Zn} and μ_{O} as the chemical potentials of zinc and oxygen, respectively, the ZnO chemical potential is:

$$\mu_{\text{ZnO}} = \mu_{\text{Zn}} + \mu_{\text{O}}. \quad (2)$$

Since the formation enthalpy of ZnO is defined as:

$$\Delta H^{\text{ZnO}} = E_{\text{ZnO}}^{\text{tot}} - \mu_{\text{Zn}} - \mu_{\text{O}}, \quad (3)$$

the potential energy of oxygen can be expressed as

$$\mu_{\text{O}} = \mu_{\text{O}_2} + \lambda \Delta H^{\text{ZnO}}. \quad (4)$$

Here μ_{O_2} is the oxygen molecule chemical potential and λ is 0 (1) for oxygen rich (poor) conditions. Furthermore, we define the chemical potential of cobalt oxide as:

$$\mu_{\text{CoO}} = \Delta H^{\text{CoO}} + \mu_{\text{Co-bulk}} + \mu_{\text{O}_2}, \quad (5)$$

where ΔH^{CoO} is the formation enthalpy of cobalt oxide bulk. Finally, the chemical potential for cobalt can be written as:

$$\mu_{\text{Co}} \leq \Delta H_{\text{CoO}} + \mu_{\text{Co-Bulk}} - \lambda \Delta H^{\text{ZnO}}. \quad (6)$$

The total energy for the respective zinc and cobalt bulk systems were calculated using a hcp crystal structure. We find a value of $\Delta H^{\text{ZnO}} = 2.88 \text{ eV}$ using PBE, which is in good agreement with other GGA calculations [35, 36]. Cohesive energies of $E_{\text{c,PBE}}^{\text{ZnO}} = -7.37 \text{ eV}$ and $E_{\text{c,PBE}}^{\text{Zn}} = -1.11 \text{ eV}$ have been calculated, which agree very well with experimental values of $E_{\text{c,exp}}^{\text{ZnO}} = -7.52 \text{ eV}$ [37] and $E_{\text{c,exp}}^{\text{Zn}} = -1.35 \text{ eV}$ [38], respectively.

Table I displays the calculated formation energies for the investigated defects under O-rich and O-poor conditions. Cobalt in ZnO has a low formation energies for both conditions in the absence of intrinsic defects (-0.91 eV, 0.94 eV). Oxygen vacancies also have a low formation energy (0.85

TABLE I. Formation energies E_f for the intrinsic defects and defect complexes in ZnO calculated with the PBE functional.

defect	E_f [eV]	
	O-rich	O-poor
Co_{Zn}	-0.91	0.94
V_{Zn}	1.63	4.51
V_{O}	3.74	0.85
Zn_{i}	5.44	2.56
O_{i}	4.01	6.89
$\text{Co}_{\text{Zn}} + \text{V}_{\text{Zn}}$	0.25	4.99
$\text{Co}_{\text{Zn}} + \text{V}_{\text{O}}$	3.41	2.37
$\text{Co}_{\text{Zn}} + \text{Zn}_{\text{int}}$	14.79	13.76
$\text{Co}_{\text{Zn}} + \text{O}_{\text{int}}$	1.83	6.57

eV) under O-poor conditions, whereas zinc vacancies have a higher formation energy (1.63 eV) under O-rich conditions. In the limit of O-rich conditions, oxygen interstitials are also more likely to form compared to the O-poor case. The opposite is true for zinc interstitials. These values agree with previous works [33, 39, 40]. On the other hand, incorporating cobalt at interstitial sites is unfavourable due to the strain and will not be discussed further [41].

The most stable defect complexes under O-rich (Zn-poor) conditions are the $\text{Co}_{\text{Zn}} + \text{V}_{\text{Zn}}$ (0.25 eV) and the $\text{Co}_{\text{Zn}} + \text{O}_{\text{int}}$ (1.83 eV) defect complexes. So it is energetically more favourable to create a zinc vacancy than to create an oxygen interstitial. This might be due to the fact that because of their size, incorporating an O atom at an interstitial site causes more stress to the ZnO matrix. This is corroborated by the observation, that $\text{Co}_{\text{Zn}} + \text{Zn}_{\text{int}}$ complexes have very high formation energies under both conditions and are therefore very unlikely to form. A possible explanation for the stability of the $\text{Co}_{\text{Zn}} + \text{O}_{\text{int}}$ complex could be the low diffusion barrier for oxygen interstitials [39]. Moreover, under O-poor (Zn-rich) conditions, only the $\text{Co}_{\text{Zn}} + \text{V}_{\text{O}}$ complex has a fairly low formation energy (2.37 eV). Interestingly, the isolated oxygen interstitial has a fairly high formation energy. This means that once it is formed during an experiment, it can quickly form complexes in the material. Since oxygen octahedral interstitials have a relatively low diffusion barrier[31, 40], it is likely to be produced under O-rich conditions and to form a stable complex.

Finally, in an attempt to give some insight in ferromagnetic properties of Co doped ZnO we briefly discuss the magnetic moments of the isolated Co defect and the Co defect in the presence of an oxygen interstitial. Much has been discussed about electron mediated ferromagnetism in transition metal doped ZnO. The energy position of the t^2 minority states relative to the host conduction band is crucial for the carrier-mediated ferromagnetism [8]. In Co_{Zn} we found an overall magnetic moment of $3\mu_B$ per Co atom. In this case no strong overlap between the Zn-4s and Co- d states is found. This means that such defect alone is unlikely to promote ferromagnetism in ZnO. On the other hand, our results show that an enhancement of the overlap between Zn-4s CBM states and Co- d states can be achieved by tuning the growth conditions where an excess of oxygen is provided [1]. This is provided by the $\text{Co}_{\text{Zn}} + \text{O}_{\text{int}}$ defect, where the Co minority t_2 states are located close to the CBM with a strong overlap with Zn-4s states. In this case, the total magnetic moment of the complex is $2.8 \mu_B$, determined by a magnetic moment of $1.92 \mu_B$ on the cobalt, $0.2 \mu_B$ on the oxygen interstitial atom, and smaller contributions from the oxygen atoms surrounding the defect complex. We propose that this scenario could favor ferromagnetism in Co doped ZnO [2–7].

In conclusion, we have performed density-functional theory and GW calculations to investigate the influence of neutral intrinsic defects in Co-doped ZnO. We find that a defect involving a cobalt atom substituting a zinc atom in the presence of an oxygen interstitial is the most probable defect giving rise to the intra- $3d$ luminescence of recent experimental finds [1]. Furthermore, we suggest that such a defect complex could help promoting ferromagnetism in cobalt doped ZnO samples.

A. L. R. and Th. F. acknowledge funding by the DFG research group FOR 1616 “Dynamics and Interactions of Semiconductor Nanowires for Optoelectronics”. A. L. R. also thanks the brazilian funding agencies CNPq and FAPEG and CENAPAD for computational resources. We thank C. Ronning, S. Geburt and M. Zapf for fruitful discussions.

-
- [1] R. Röder, M. Zapf, S. Geburt, D. Franke, M. Lorke, A. L. da Rosa, T. Frauenheim, and C. Ronning, *phys. stat. sol. (b)* **256**, 1800604 (2019).
 - [2] I. Djerdj, Z. Jagličić, D. Arčon, and M. Niederberger, *Nanoscale* **2**, 1096 (2010).
 - [3] I. A. Sarsari, C. D. Pemmaraju, H. Salamati, and S. Sanvito, *Phys. Rev. B* **87**, 245118 (2013).
 - [4] R. Janisch, P. Gopal, and N. A. Spaldin, *Journal of Physics: Condensed Matter* **17**, R657 (2005).

- [5] H. A. Weakliem, The Journal of Chemical Physics **36**, 2117 (1962).
- [6] K. C. Verma and R. K. Kotnala, Phys. Chem. Chem. Phys. **18**, 17565 (2016).
- [7] W. Li, G. Wang, C. Chen, J. Liao, and Z. Li, Nanomaterials **7**, 20 (2017).
- [8] I. A. Sarsari, C. D. Pemmaraju, H. Salamati, and S. Sanvito, Phys. Rev. B **87**, 245118 (2013).
- [9] A. L. Schoenhalz and G. M. Dalpian, Phys. Chem. Chem. Phys **15**, 15863 (2013).
- [10] C. H. Patterson, Phys. Rev. B **74**, 144432 (2006).
- [11] K. Yim, J. Lee, D. Lee, M. Lee, E. Cho, H. S. Lee, H.-H. Nahm, and S. Han, Sci. Rep. **7**, 40907 (2017).
- [12] S. Das Sarma, American Scientist **89**, 516 (2001).
- [13] R. Feynman, Foundation of Physics **16**, 507 (1986).
- [14] C. Ronning, C. Borschel, S. Geburt, R. Niepelt, S. Müller, D. Stichtenoth, J. P. Richters, A. Dev, T. Voss, L. Chen, et al., physica status solidi (b) **247**, 2329 (2010), ISSN 1521-3951, URL <http://dx.doi.org/10.1002/pssb.201046192>.
- [15] S. Geburt, M. Lorke, A. L. da Rosa, T. Frauenheim, R. Röder, T. Voss, U. Kaiser, W. Heimbrodt, and C. Ronning, Nano Letters **14**, 4523 (2014).
- [16] S. Geburt, R. Röder, U. Kaiser, L. Chen, M.-H. Chu, J. Segura-Ruiz, G. Martínez-Criado, W. Heimbrodt, and C. Ronning, physica status solidi (RRL) – Rapid Research Letters **7**, 886 (2013).
- [17] J. Segura-Ruiz, G. Martínez-Criado, M. H. Chu, S. Geburt, and C. Ronning, Nano Letters **11**, 5322 (2011).
- [18] Z. Jin, T. Fukumura, M. Kawasaki, K. Ando, H. Saito, T. Sekiguchi, Y. Z. Yoo, M. Murakami, Y. Matsumoto, T. Hasegawa, et al., Applied Physics Letters **78**, 3824 (2001).
- [19] C. A. Johnson, T. C. Kaspar, S. A. Chambers, G. M. Salley, and D. R. Gamelin, Phys. Rev. B **81**, 125206 (2010).
- [20] P. Hohenberg and W. Kohn, Phys. Rev. **136**, B864 (1964).
- [21] W. Kohn and L. J. Sham, Phys. Rev. **140**, A1133 (1965).
- [22] L. Hedin, Phys. Rev. **139**, A796 (1965).
- [23] G. Kresse and D. Joubert, Phys. Rev. B **59**, 1758 (1999).
- [24] P. E. Blöchl, Phys. Rev. B **50**, 17953 (1994).
- [25] J. P. Perdew, K. Burke, and M. Ernzerhof, Phys. Rev. Lett. **77**, 3865 (1996).
- [26] M. Lorke, T. Frauenheim, and A. L. da Rosa, Phys. Rev. B **93**, 115132 (2016).
- [27] D. Franke, A. L. da Rosa, M. Lorke, and T. Frauenheim, phys. stat. sol. (b) **256**, 1800455 (2019).

- [28] S. Lany and A. Zunger, Phys. Rev. B **81**, 113201 (2010).
- [29] D. Wang, G. Xing, M. Gao, L. Yang, J. Yang, and T. Wu, The Journal of Physical Chemistry C **115**, 22729 (2011), <http://pubs.acs.org/doi/pdf/10.1021/jp204572v>, URL <http://pubs.acs.org/doi/abs/10.1021/jp204572v>.
- [30] S. Lany and A. Zunger, Phys. Rev. B **81**, 113201 (2010).
- [31] A. Janotti and C. G. van de Walle, Phys. Rev. B **76**, 165202 (2007).
- [32] S. J. Clark, J. Robertson, S. Lany, and A. Zunger, Phys. Rev. B **81**, 115311 (2010), URL <http://link.aps.org/doi/10.1103/PhysRevB.81.115311>.
- [33] S. Lany and A. Zunger, Phys. Rev. B **81**, 113201 (2010).
- [34] C. G. Van de Walle and J. Neugebauer, Journal of Applied Physics **95**, 3851 (2004).
- [35] F. Oba, A. Togo, I. Tanaka, J. Paier, and G. Kresse, Phys. Rev. B **77**, 245202 (2008).
- [36] S. B. Zhang, S.-H. Wei, and A. Zunger, Phys. Rev. B **63**, 075205 (2001).
- [37] W. M. Haynes, ed., *CRC handbook of chemistry and physics: A ready-reference book of chemical and physical data* (CRC Press, Boca Raton, 2016), 97th ed.
- [38] E. Kaxiras, *Atomic and Electronic Structure of Solids* (Cambridge University Press, Cambridge, 2003).
- [39] A. Janotti and C. G. Van de Walle, Phys. Rev. B **76**, 165202 (2007).
- [40] G.-Y. Huang, C.-Y. Wang, and J.-T. Wang, J. Phys.: Condens. Matter. **21**, 195403 (2009).
- [41] G. S. Chang, E. Z. Kurmaev, D. W. Boukhvalov, L. D. Finkelstein, S. Colis, T. M. Pedersen, A. Moewes, and A. Dinia, Phys. Rev. B **75**, 195215 (2007).

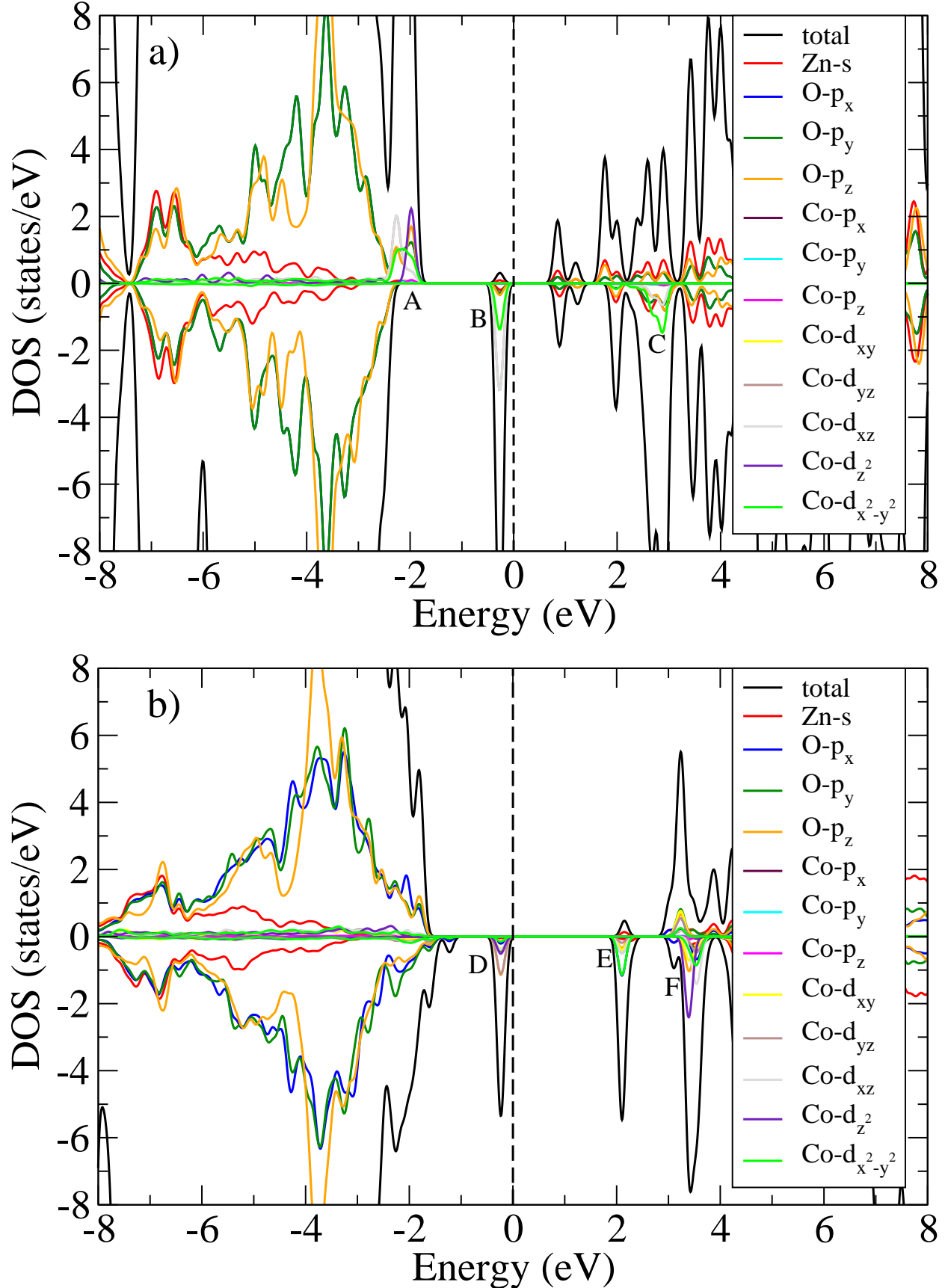


FIG. 2. Orbital projected density of states calculated within the PBE+GW₀ approximation for a) CoZn : A denotes states close to VBM, B denotes states close to the Fermi level and C denotes states close to the CBM and for b) $\text{CoZn} + \text{O}_{\text{int}}$: D are states close to the Fermi level, E are states close to CBM and F are higher

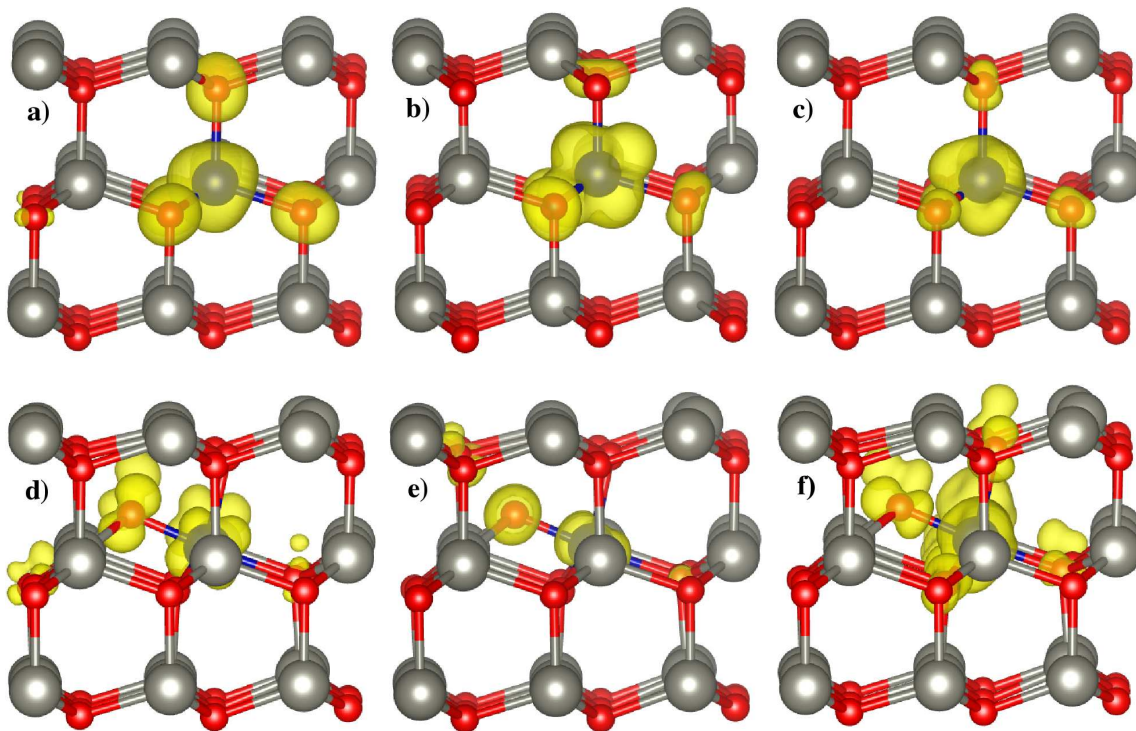


FIG. 3. Band projected charge density for the CoZn and $\text{CoZn} + \text{O}_{\text{int}}$ complexes calculated within the PBE+ GW_0 approximation for CoZn : a) VBM (states located at A), b) states close to the Fermi level (states located at B), c) states located at C; and for $\text{CoZn} + \text{O}_{\text{int}}$: d) states close to the Fermi level, e) states located at E and f) higher states in the conduction band located at F. The corresponding states A-F are shown in Fig. 2. Isosurface values are $0.005e/\text{\AA}^3$.

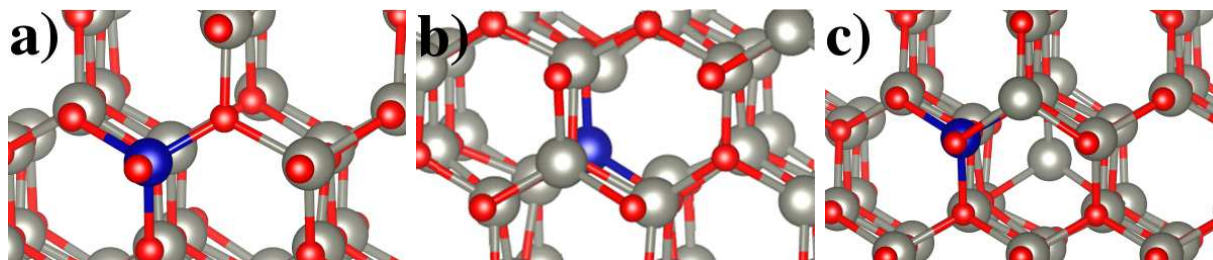


FIG. 4. Atomic structure around the a) $\text{CoZn} + \text{V}_{\text{Zn}}$, b) $\text{CoZn} + \text{V}_{\text{O}}$ and c) $\text{CoZn} + \text{Zn}_{\text{int}}$ complexes calculated with the PBE functional. Grey, red and blue spheres represent Zn, O, and Co atoms, respectively.

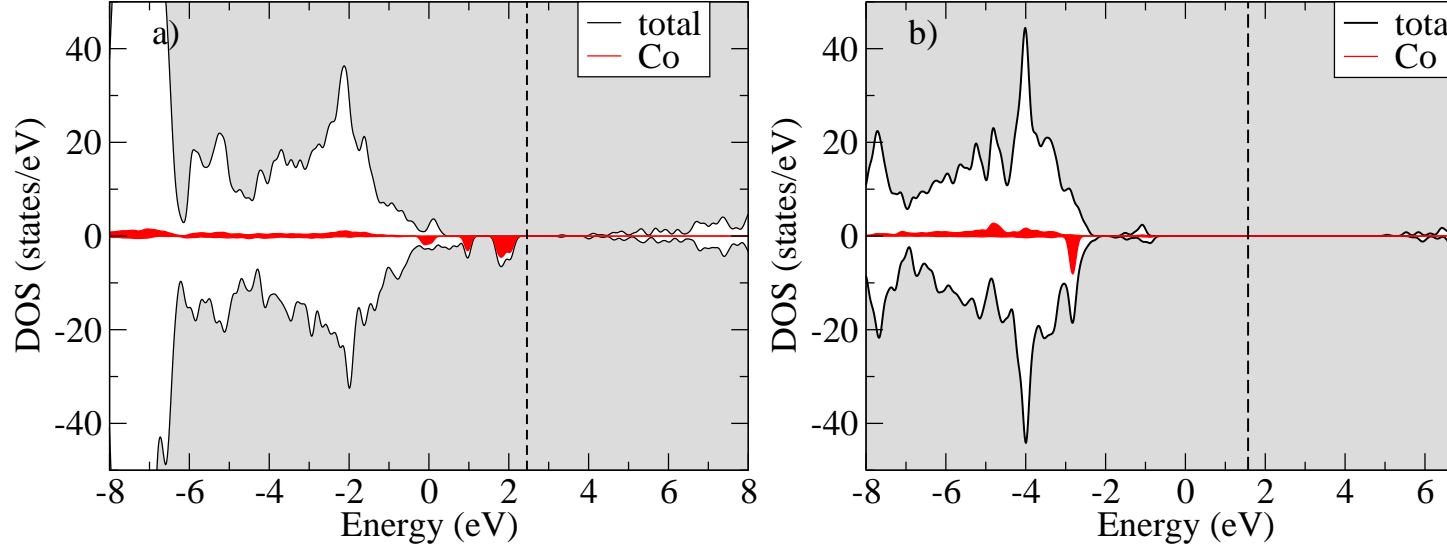


FIG. 5. Total and atom projected density of states for a) $\text{CoZn} + \text{V}_{\text{Zn}}$, b) $\text{CoZn} + \text{V}_{\text{O}}$ and c) $\text{CoZn} + \text{Zn}_{\text{int}}$ complexes calculated within the PBE+ GW_0 approximation. The vertical line denotes the highest occupied state. Positive (negative) values of the DOS denote spin up (down).